

Experimental study of the hydromechanical response and liquefaction susceptibility of nickel ore to maritime transportation

Pascal Bigarre, Jean-Bernard Kazmierczak, S. Collignon

▶ **To cite this version:**

Pascal Bigarre, Jean-Bernard Kazmierczak, S. Collignon. Experimental study of the hydromechanical response and liquefaction susceptibility of nickel ore to maritime transportation. 10. Asian Rock Mechanics Symposium (ARMS 10) - ISRM International Symposium for 2018, Oct 2018, Singapore, Singapore. ineris-03239685

HAL Id: ineris-03239685
https://ineris.hal.science/ineris-03239685

Submitted on 27 May 2021

HAL is a multi-disciplinary open access archive for the deposit and dissemination of scientific research documents, whether they are published or not. The documents may come from teaching and research institutions in France or abroad, or from public or private research centers.

L'archive ouverte pluridisciplinaire **HAL**, est destinée au dépôt et à la diffusion de documents scientifiques de niveau recherche, publiés ou non, émanant des établissements d'enseignement et de recherche français ou étrangers, des laboratoires publics ou privés.

Experimental Study of the Hydromechanical Response and Liquefaction Susceptibility of Nickel Ore to Maritime Transportation

P. Bigarré[a]*, J.B. Kazmierczak[a] and S. Collignon[b]

[a] *National Institute for Industrial Environment and Risks, Verneuil-en-Halatte, France*
[b] *Société Le Nickel, Nouméa, New Caledonia*
* pascal.bigarre@ineris.fr

Abstract

When transported in ship carriers nickel ore with excessive humidity may exceed its flow moisture point and liquefy under the effect of cyclic ship motion induced by the swell. Liquefaction of solid bulk means that the material loses all internal strength and behaves as a liquid. Once the phenomenon happens in one or several holds, the vessel is potentially unstable and may capsize very fast.

The Flow Moisture Point, and then the Transport Moisture Limit, depend on several physical properties of the bulk mineral ore, among which its moisture content, of course, but also the amount of cyclic shear stresses exerting in the mass of ore during its maritime transportation.

With the purpose to ascertain this key parameter so-called Cyclic Shear Ratio (CSR) to be considered when calibrating TML tests from triaxial tests in laboratory, a handysize bulk carrier was instrumented inside its nickel ore cargo with a multi-parameter monitoring system aiming to sample dynamic stresses versus ship motion and sea conditions. The authors detail here below this unique experiment based on two sea passages from New Caledonia to Japan and the principal observations and results obtained.

Keywords: Nickel Ore, Liquefaction, Dynamic Stress Monitoring, Sea Passage Experiment

1 Introduction

1.1 Context

When transported in ship carriers, nickel ore with excessive humidity, as many other solid bulk cargos, may exceed its flow moisture point and liquefy under the effect of the cyclic ship motion induced by the swell. Liquefaction means that the solid bulk loses all internal strength and behaves as a liquid. Once the phenomena happen in one or several holds, the vessel is potentially unstable and may capsize very fast (Sheng, 2012).

Numerous dramatic shipwrecks have been reported worldwide those past decades due to the liquefaction of solid bulk cargoes. Recall that in 2010, the majority of bulk carrier deaths were attributed to cargo liquefaction. This is most likely what happened in 2010 at the origin of the shipwrecks of the Jian Fu Star (October 27, 2010 - 13 dead), the Nasco Diamond (November 10, 2010 - 21 dead) and the Hong Wei (December 3, 2010 - 10 dead). It should be noted, however, that the nickel ores transported in these vessels did not come from New Caledonia.

Based on the International Maritime Organization's work, the IMSBC code entered into force on 1 January 2011. This code establishes the conditions for maritime transportation of solid bulk cargos, including issues relating to products susceptible to liquefaction. These products are listed into the so-called group A in the "individual sheets of bulk cargoes" in Appendix 1 of the Code. Besides Nickel Concentrate, “Nickel Ore” has officially included this group and therefore cannot be transported by ship if its effective moisture content is greater than or equal to its TML. The IMSBC Code states that the shipper shall provide the ship’s master or his representative with a signed certificate that must contain or be accompanied by the results of the TML testing determined as 90% of the Flow Moisture Point (FMP) and the water content of the loaded solid bulk.

1.2 New Caledonia situation

With a production of more than 16.500 kth in 2017, New Caledonia is one of the major worldwide producer and exporter of nickel ore. While the ore is transported from the mine sites to the plants by ship along the coast, New Caledonia exports also routinely nickel ore by ship to Asia and Australia. The Union of Ore Exporters of New Caledonia (SEM in French) was very soon fully concerned by the design and the effectiveness of an operational test of the TML to guarantee the maritime transportability of its ore and ensure its capability to deliver the required certificates.

Recall that the IMSBC code recommends three laboratory test methods that can determine the moisture content limit for a given ore raked in the A group. These are the flow table test, the penetration test and the Proctor / Fagerberg test methods. Nonetheless, all three methods being limited to fine particle size ores, the SEM undertook a research program to design a customized FML-TML test well adapted to their large grain size ores.

A thorough analysis of the three tests proposed showed that the vibrating table with penetrometer bit test (so-called VTPB) was the one that, although to be adapted, presented as the most promising to design such an operational reliable TML test. In fact, the dimensions of the ore sample (200 mm in diameter) allow high particle sizes and the penetration principle associated with vertical vibrations makes it possible to simulate a cyclic shear solicitation. By the way, considering the variable properties and the natural humidity of the laterites and saprolites in New Caledonia, a first design of the FML/TML test based on a Cyclic Shear Ratio fixed thanks to numerical modelling study ended as too severe, rejecting numerous samples of nickel ore known to be transportable.

2 Liquefaction phenomenon

2.1 Cyclic Shear Ratio

Besides physical properties as moisture content, density and grain size distribution, a key criterion to quantify liquefaction susceptibility is related to the Cyclic Shear Ratio (CSR) exerting in a finite representative volume of humid ore, that is the ratio of the CSR to the average consolidation stress of this volume of ore.

The CSR develops from the movement of the ship, rearranging soil particles and reducing steadily the volume of spaces between those (as mechanical vibrations compact loose soils), causing the pore water pressure to rise and reducing thereby the shear strength of the bulk. Pore water pressure refers to the pressure of water held within a soil or rock, in gaps between particles, i.e. pores. If the pore water pressure increases enough, the solid bulk cargo can reach its flow moisture point. The cargo enters a stage of transition whereby it begins to react like a fluid because of the loss of friction between the particles. This process is like the ground liquefaction physical process occurring in some extended urban areas shaked by seismic strong ground motion during a few tens of seconds. This phenomenon is extensively documented along with numerous impressive videos on the internet.

In this study, the CSR, $\kappa(t)$, is defined in fact as the ratio between the dynamic part of the shear stress to the average, $q(t)$-qo, and p'(t) the average total effective stress. Here we have:

$$\kappa(t) = \frac{q(t) - q_0}{2.p'(t)} \tag{1}$$

$$q(t) = \sqrt{\sigma_{xx}^2 + \sigma_{yy}^2 + \sigma_{zz}^2 + 3\left(\sigma_{xz}^2 + \sigma_{xy}^2 + \sigma_{yz}^2\right) - \sigma_{xx}\sigma_{zz} - \sigma_{yy}.\sigma_{zz} - \sigma_{yy}\sigma_{xx})} = \sqrt{3J_2} \tag{2}$$

$$p'(t) = \frac{\sigma'_{xx} + \sigma'_{yy} + \sigma'_{zz}}{3} = \frac{I_1}{3} \tag{3}$$

With I1 and J2 the two invariants of the stress tensor [σ]:

$$[\sigma] = \begin{bmatrix} \sigma_{xx} & \sigma_{xy} & \sigma_{xz} \\ \sigma_{yx} & \sigma_{yy} & \sigma_{yz} \\ \sigma_{xz} & \sigma_{yz} & \sigma_{zz} \end{bmatrix} \quad (4)$$

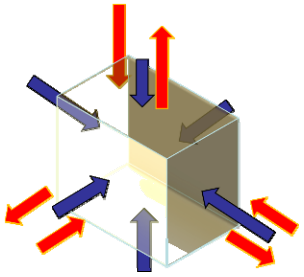


Fig. 1: Schematic illustration of a representative volume of ore on which isotropic stresses (blue) and shear stresses (red) are exerting with both quasi-static and dynamic regimes. While the swell rises during maritime transportation, the superimposed dynamic stresses may induce compaction, with excess pore pressure rising progressively and potentially triggering liquefaction. From equations above, one can see that a high value of the total effective stress p' calls for higher dynamic shear stresses to trigger the liquefaction. On the opposite, unstressed solid bulk, close to the free surface of a ore pile, may liquefy as soon as the dynamic shear stress appears.

Recall that for a plane perpendicular to Oxy and oriented at 45° from 0x and 0y, the stress components σ_{xx}, σ_{yy} , σ_n and τ_{xy} are related as follows:

$$\tau_{xy} = \sigma_n - 0.5 \cdot \sigma_{xx} - 0.5 \cdot \sigma_{yy} \quad (5)$$

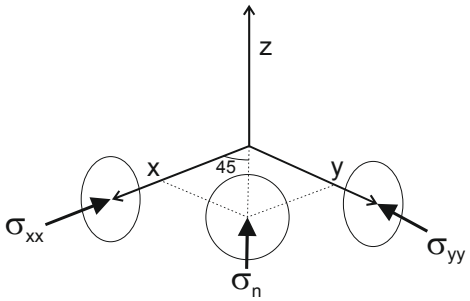


Fig. 2: schematic representation of three normal stresses perpendicular lying in the oxy plane, 45° apart one from each other. From $\sigma_{xx}(t)$, $\sigma_{yy}(t)$ and $\sigma_n(t)$, the shear stress $\tau_{xy}(t)$ may be processed from equation (6).

Equation (6) may be extended to τ_{xz} and τ_{yz} in relation with two other normal stresses σ_n lying 45° in 0xz and 0yz. So, extending Fig. 2 along with equation $\tau_{xy} = \sigma_n - 0.5 \cdot \sigma_{xx} - 0.5 \cdot \sigma_{yy}$ (5) to a set of six continuously monitored TPCs adequately positioned, it is possible to track the full time dependent stress tensor $[\sigma]$, in both its quasi-static and dynamic components. Once $[\sigma]$ time series processed, one can derive from equation (1) to (3) $q(t)$, $p'(t)$ and then the CSR $\kappa(t)$.

2.2 Measurement of the stresses and the CSR

Total Pressure Cell (TPC) is a well-known sensor made of two circular plates of stainless steel welded together to form a very flat sealed cavity filled with fluid and connected to a pressure

transducer. Once installed in the soil, the total pressure acting on the surface is transmitted to the fluid and measured by the pressure transducer. Pressure measurements in loose soils are usually made with total pressure cells, widely used since decades for this purpose in civil engineering and soil mechanics (Valentin, 2001).

Among the important specifications to be accounted for, a distance between two cells must be at least twice the outer diameter of a cell, that is 65 cm for 32 cm diameter TPC, to limit significant inter-influence. A second usual recommendation is to bury the cell into a loose soil with fine particles to ensure homogeneous application of the pressures on its flat sensitive surface, respecting a 1 to 10 ratio condition between granular size and diameter of the cell.

According to those recommendations, a specific metallic frame was designed to implement and bury adequately a set of six oriented TPCs. 0-30 mm sieved ore was prepared to bury each set of sensors.



Fig. 3 Left: schematic of a cluster of six total pressure cells positioned and oriented relatively one to each other: 3 vertical, 1 horizontal, 2 inclined. TPCs are fixed to the frame with clamps. Right: picture of the system, carefully positioned and hand compacted with a layer of sieved ore before removal of the clamps and the frame.

Dimensions of the triangular frame were 1.5mx1.5m to be compared to the 25mx26m basement of the around 10 meters high pile of ore in each hold. These mean that the volume of ore in the immediate vicinity of a cluster of sensors may be considered small enough to admit a constant stress field as soon as the cluster is at least a few meters from the free surface inside the ore pile.

2.3 Design and implementation of the instrumentation

Since the stress field in an ore pile filling a hold has gradients from the free surface towards the center of the basement, it was necessary to measure the CSR at different positions inside the solid bulk. Two holds among the five were then instrumented with a total of six TPCs clusters. The second hold from the bow was instrumented with five clusters distributed in the ore pile, while the fifth hold close to the after castle was instrumented for benchmark purposes with one cluster. All TPCs clusters were implemented progressively during the loading process that last a few days, taking advantage of the necessity to load the holds progressively and alternatively to keep the ship at equilibrium. From there the successive steps were first to prepare a flat surface at a predetermined location, to position and bury partially the TPCs cluster completed with two water content sensors, three accelerometers and one temperature gauge, all sensors cabled to a monitoring unit buried close. Once the whole set of sensors connected to the digital recorder, the latter was then cabled to a central monitoring unit installed in one of the mast house on the deck. Once analogue acquisition and digital data transmission fully tested, the clamps and metallic frame were carefully removed, the system fully hand-compacted with sieved ore before careful resumption of the usual loading process of the hold with the grab crane.



a



b



c



d

Fig. 4 a- handsize carrier with its four grab cranes deserving the five holds. b- preparation of a flat surface to install a cluster of sensors. c- marking out the buried set of sensors for easy retrieval of the equipment at destination port. d- resumption of the loading process of the hold with the grab crane.

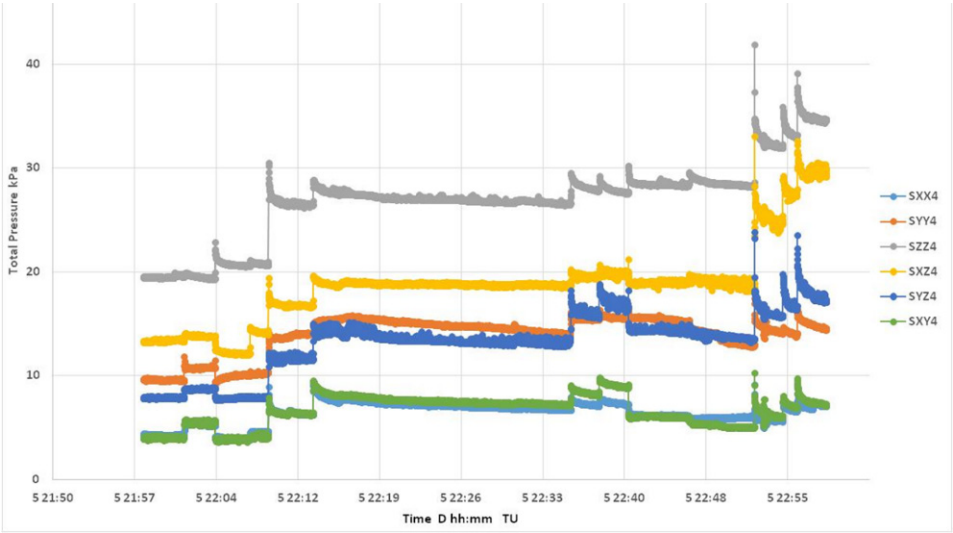


Fig. 5: time series of a TPCs cluster soon after its installation in the ore pile. Spikes and pressure increments show the impact of the ore released by the grab crane. The maximum pressure recorded is vertical, based on the horizontally placed TPC σ_{zz} (gray). Local stress field is clearly anisotropic.

3 Other measurements

3.1 Water content and pore pressure measurements

Although the ore used was known to be unsaturated, two water content sensors completed each TPCs cluster and two isolated pore pressures sensors were set up in the solid bulk to monitor potential fluctuations in the negative pressure domain. In other words, it was assumed early in the design of the experiment, and measurements obtained proved this as a correct assumption, that total pressure measured by the TPCs were effective pressures.

3.2 Complementary on-board measurements

Besides the six buried TPCs clusters buried in the ore, the instrumentation included also a water level sensor set up in the bilge well to detect and quantify the amount of pore water evacuating from the ore pile, three radar distance-meters to monitor residual compaction of the ore pile and a Motion-Response Unit (MRU) measuring accurately the reference ship motion. On-board MRU enables to record the six accelerations and rotation components, along with the on-line processing of the heave. Eventually other sensors as atmospheric pressure, outside temperature and GPS to position the ship all along its sea passage completed the system.

In total 84 sensors were installed and monitored continuously at different sampling frequencies: 2Hz for most geotechnical sensors, 1 kHz for seismic accelerometers and 10 minutes for the GPS, the radar distance-meters, the outside temperature and the atmospheric pressure.

4 The experiments

Two similar experiments were conducted each of them during a 14 days sea passage from New Caledonia to Japan, first in September 2013 and second in April 2014. These were undertaken on the Coral Ocean handysize bulk carrier from Daichi Corporation thanks to a collaborative agreement with the SEM. Coral Ocean is a 33.000 DWT, 172 m long vessel launched in 2012. Two experiments were considered useful to increase both robustness of the dataset to be collected and to enlarge the encountered sea conditions.

The Nickel ore used for these two experiments is known as Bonini nickel ore. It has been described and characterized by the CERMES laboratory, France, with high clay content and an average humidity H of the ore for the two passages measured as follows:

Sea passage 1: H = 27,5% and Sea Passage 2: H = 24%, with a TML measured at 33,13%

5 Weather and sea conditions during the experiments

5.1 Observed swell

During the first sea passage SP1, the crew noted on a two hours basis the swell level and the swell direction on a logbook. The time series showed clearly three periods with significant or high swell: first day after departure, and four days later. If these data were not recorded by the crew during sea passage SP2, the sea conditions were reported much quiet than during SP1.

5.2 Ship motion

Swell characterizes the sea conditions, from calm to very high, and sea conditions induce the ship motion that can be well quantified thanks to the reference MRU. Among many others, three important parameters to quantify this cyclic motion and then the sea conditions are as follows:

1. the Excess acceleration rate, E_{ar}(t), defined as the relative difference of the complete acceleration and the gravity g

$$E_{ar} = \frac{\left\| \vec{A} \right\| - \vec{g}}{\vec{g}} \tag{6}$$

2. the Heave *H(t)*, here defined as the peak-to-peak height following the z motion of the ship
3. the Roll *R(t)* of the ship, here defined as the 0-to-peak tilt around the longitudinal axis of the ship

These are described here below.

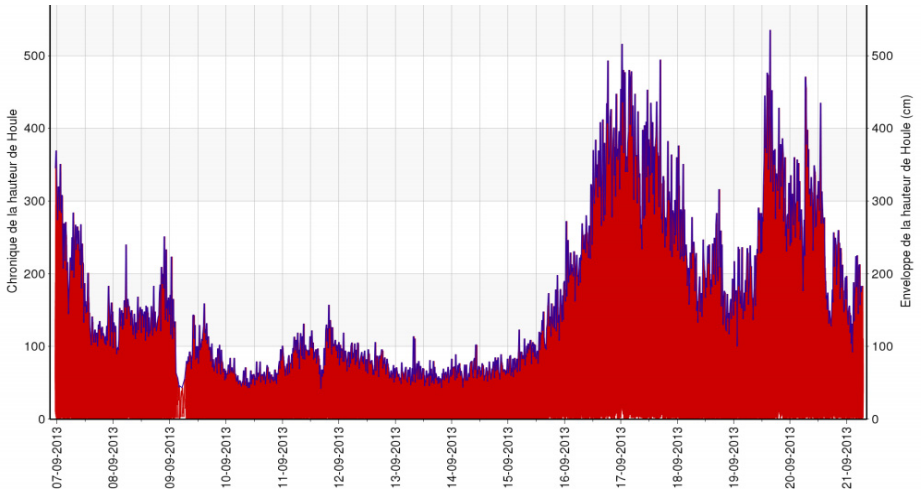


Fig. 6: Vertical axis: Time series of the reference heave $H(t)$, red, sea passage 1, and the maximum reference heave $H_m(t)$ calculated on successive time windows of 15 minutes during the 14 days of sea passage 1, blue. Apparent discrepancy between $H(t)$ and $H_m(t)$ is due only to graphical limitations of out-of-range number of values for $H(t)$.

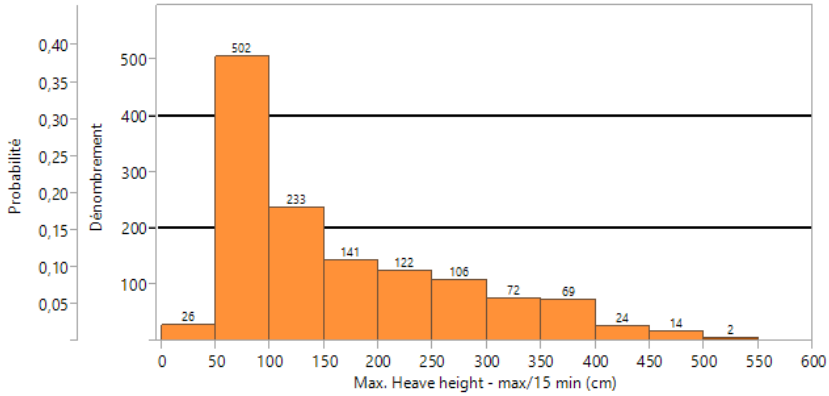


Fig. 7: right-skewed distribution of the maximum heave $H_m(t)$ calculated on successive time windows of 15 minutes during the 14 days of sea passage 1. Vertical axis: counting and probability, horizontal axis: classes of values.

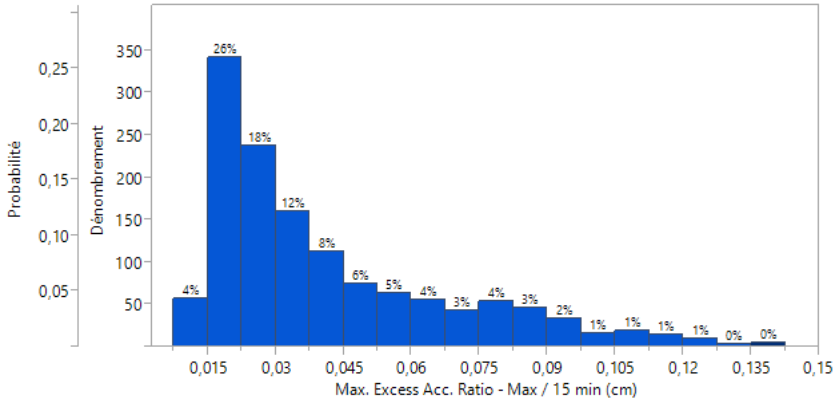


Fig. 8: right-skewed distribution of the maximum reference E_{ar} calculated on successive time windows of 15 minutes during the 14 days of sea passage 1. Vertical axis: counting and probability, horizontal axis: classes of values.

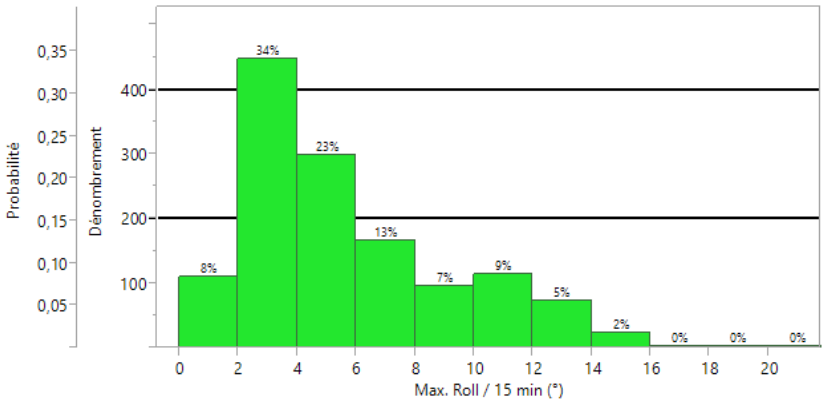


Fig. 9: right-skewed distribution of the maximum reference roll position *Rm(t)* calculated on successive time windows of 15 minutes during the 14 days of sea passage 1. Vertical axis: counting and probability, horizontal axis: classes of values.

	E_{ar} (%)		Heave (cm)		Roll (°)	
	SP1	**SP2**	**SP1**	**SP2**	**SP1**	**SP2**
maximum	13,9	9,7	535	355	20,3	11,8
mediane	4	3,5	126	117	4,6	4,2
minimum	-	-	42	18	1,01	0,7

Table 1: statistics about Excess Acceleration Rate, Heave and Roll recorded during the two sea passages SP1 and SP2.

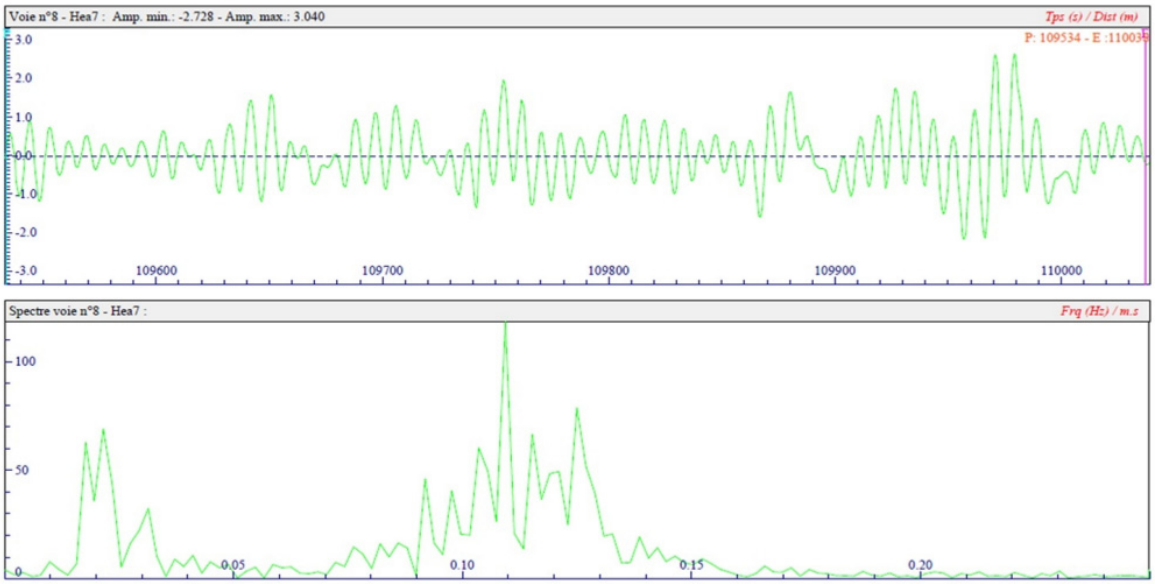


Fig. 10: above: zoom on the time series of Heave *H(t)*, during a time period of around 10 minutes, sea passage 1. A 4,5 meters peak-to-peak heave is discernable. Below: Spectral content of the signal *H(t)* showing two dominant frequencies at 0.02 Hz and 0.11 Hz, corresponding respectively to the periods of 50s and 9s.

6 Dynamic stresses and Cyclic Shear Ratio

Figure 11 shows a time window of a TPCs cluster time series with the cyclic pressure variations induced by the ship motion, the dynamic part of each pressure component acting to generate a cycle shear stress on the instrumented volume of ore.

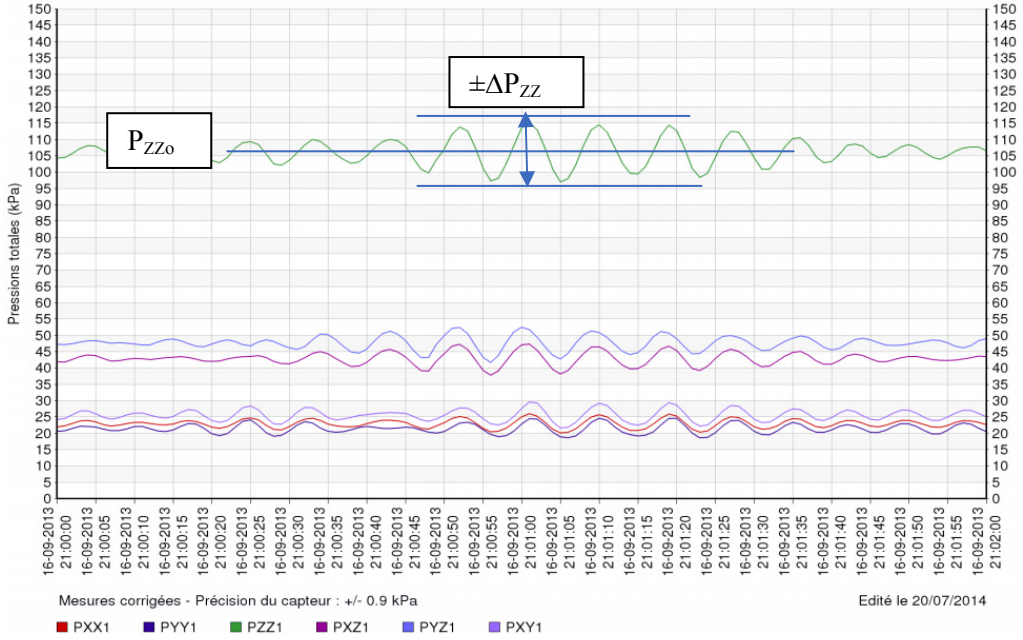


Fig. 11: zoom on a 2 minutes time window of the six TPC time series of one of the cluster, showing the dynamic total pressures induced by the ship motion. Here, the pressure Pzz is centered on Pzzo= 105 kPa, with a dynamic part of ±10 kPa. Vertical axis: pressure – kPa, horizontal axis : time.

For each TPCs clusters and the two sea passages, the time series of the stress tensor [σ] was computed. CSR time series, $\kappa(t)$, was then processed from equation (1). Since the heave motion of the ship is only one component of the complex motion of the ship, the derived heave time series H(t) and CSR time series $\kappa(t)$ from the measurements are not in phase, rendering any direct correlation analysis of no-use due to the high level of dispersion obtained. A simple way to circumvent this difficulty is to analyze the time series of the maximum values calculated for each successive 15 minutes time window, based on the reasonable consideration that any finite time window with low or high heave is expected to show respectively low or high dynamic stresses and then low or strong CSR.

6.1 Cyclic shear ratio Distributions

Distributions of the maximum CSR of one of the TPCs clusters is shown in Fig. 12 for the two experiments. Distributions are different since the sea conditions encountered were not the same.

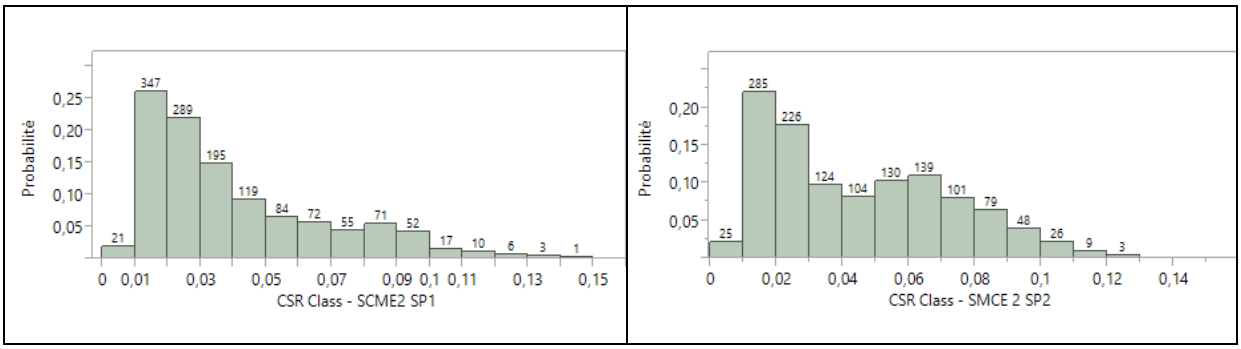


Fig. 12: right-skewed distribution of the maximum CSR $\kappa_m(t)$ for one TPCs cluster calculated on successive time windows of 15 minutes during the 14 days of sea passage 1, left, and sea passage 2, right. Vertical axis: probability, horizontal axis: classes of values.

6.2 Cyclic shear ratio versus heave

Regression analysis of the Maximum Cyclic Shear Ratio and Maximum Heave for one TPCs cluster during sea passage 1 is shown in Fig. 13 here below.

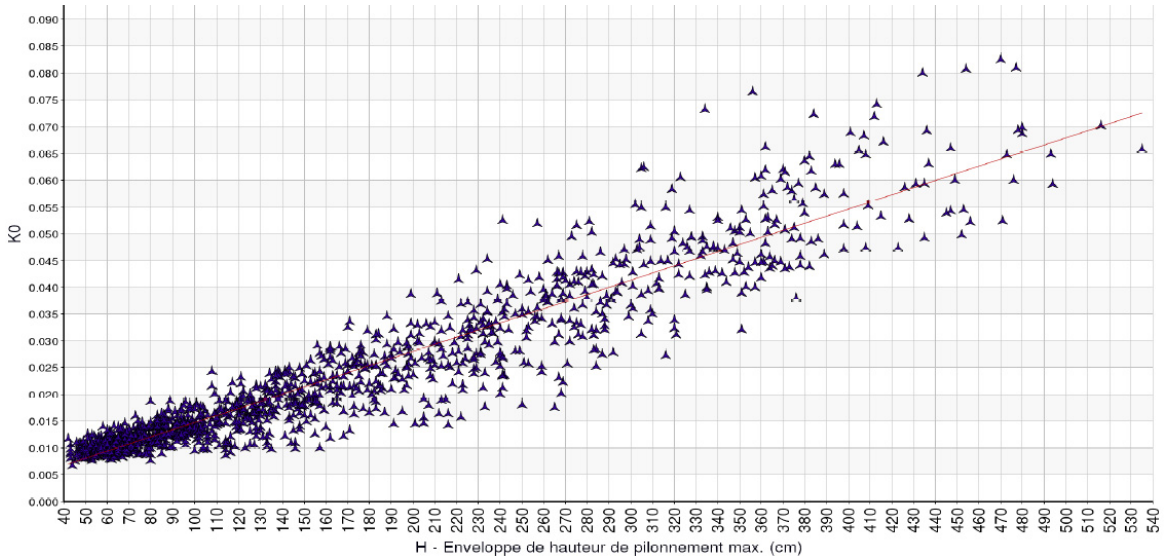


Fig. 13: XY correlation plot of maximum CSR $\kappa_m(t)$, vertical axis, and maximum heave $H_m(t)$ for one TPCs cluster, horizontal axis (m), sea passage 1. The dispersion increases with higher values.

The plot shows a clear linear trend between the two variables along with a heteroscedastic character. This increasing dispersion is most likely due to the increasing complexity of the true 3D ship motion, for which heave is only one part, with worsening sea conditions, for which dynamic stress tensor carries more complete information. Heteroscedasticity may be usually corrected using two common techniques:

1. View logged outcome data. Variability appears as increasing, but the variability in percentage terms may be rather stable. The CSR Y-variable may be transformed into the Log (CSR) Y-variable
2. Use a different specification for the predicting variable. here, we propose to transform the Heave X-variable into the Squared Heave X –Variable. In this case, this transformation refers to the potential energy of the ship rather than to his amplitude of vertical motion.

The transformed regression is shown in figure 14 here below.

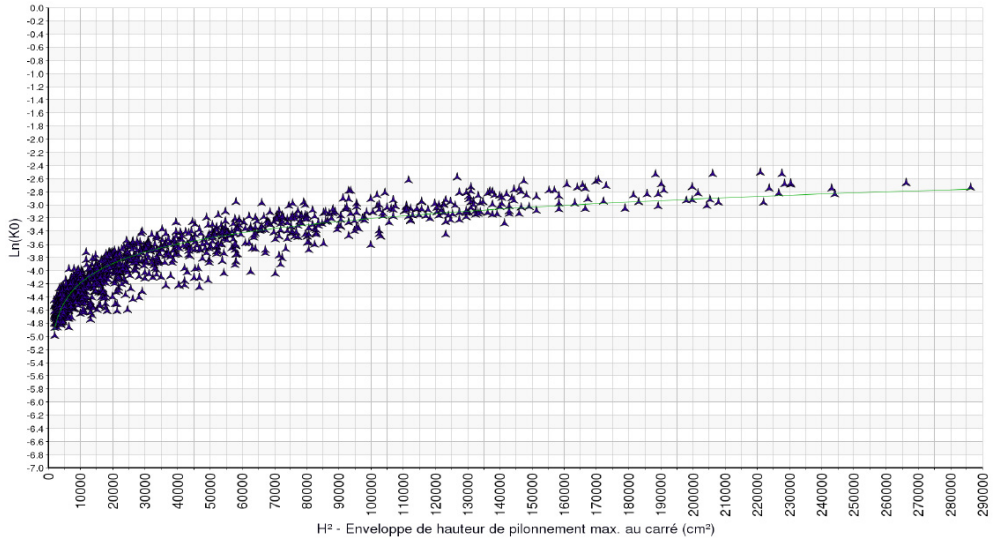


Fig. 14 : XY correlation plot of the transformed variables Log($\kappa_m(t)$), vertical axis, and $H_m(t)^2$ for one TPCs cluster, horizontal axis (m), sea passage 1.

7 Main results

From the data measurements obtained and observations made from the two experiments, main results obtained may be summarized as follows:

1. As expected the ship dominant motions were found to be heave, surge and roll. Sea passage 1 encountered strong sea conditions, with a maximum heave of 5.35 meters, a maximum roll close to 20°, while 3D accelerations measured at different locations never exceed 20% of gravity. These extremums values were reached during a very short period compared to the 14 days. Sea passage 2 was much quiet, with a maximum heave of 3.55 meters;
2. Maximum excess acceleration rates measured range from 10% to 19% depending of the TPCs cluster and sea passage considered;
3. Compaction of the nickel ore occurs essentially during the loading process. However, compaction has been detected and measured clearly while the sea conditions were worsening during sea passage 1. Radars detected what corresponds clearly to a quasi-static failure along with mass movement of the bulk cargo, phenomena not related to the physics of liquefaction;
4. Water content sensors measured no significant variations: no water was extracted from the bilgewater during the sea passage. This is explained by the compaction during the loading of the hold and the low permeability of the ore containing a lot of clay;
5. Data analysis shows clearly that a statistical relationship between the logarithm of the CSR and the potential energy of the cargo may be reasonably assessed. The maximum CSR reaches a value of 0.158. Extrapolation provides a maximum CSR value of 0.16 for a hypothetical 5.5-7.5-meter heave range. The CSR value of 0,16 was selected to run advanced triaxial laboratory tests undertaken to constrain the design of an adapted VTPB test.

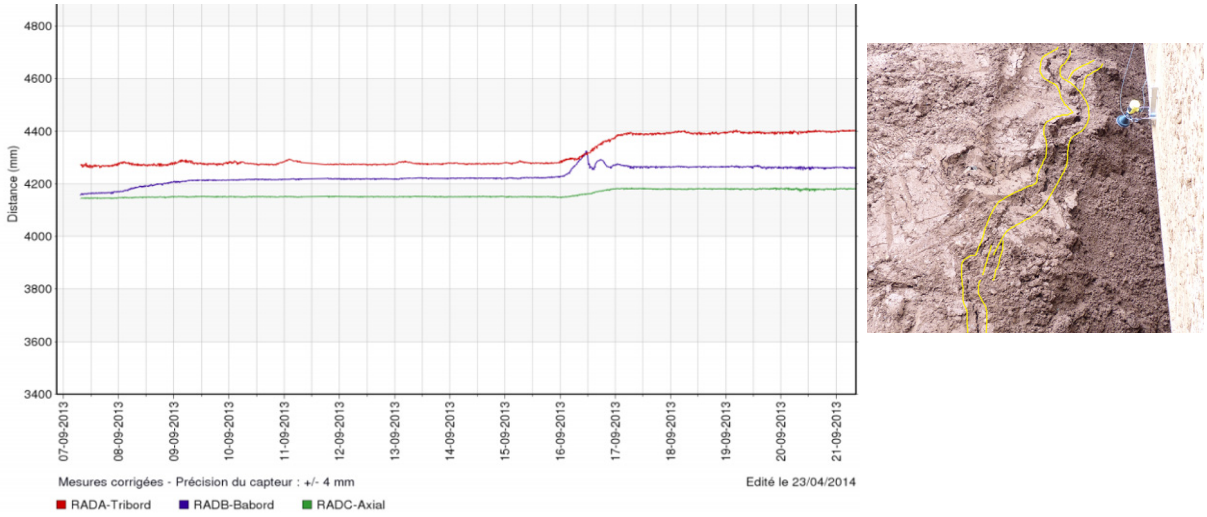


Fig. 15: left: time series of the displacement measurements over the surface of the cargo, SP 1. Vertical axis: distance in mm from the three radars to the free surface pointed at. Horizontal axis: time. Superficial sliding of the ore along with a significant mass movement is detected during the 9th day. Right: picture a long fracture, underlined in yellow, crossing the ore pile just below one of the radar distance-meter (device visible at the top right of the picture plugged on the hatch coaming).

8 Conclusions

Maritime transportation of humid solid bulk is an industrial process at risk. Among the key physical parameters that govern the liquefaction risk the Cyclic Shear Ratio exerting on the solid bulk determined its Transport Moisture Limit. CSR depends mainly on the sea conditions encountered during the sea passage and the ship itself, with a dynamic interaction difficult to assess from numerical models. This paper described an experimental approach undertaken to measure and ascertain a reliable value of the CSR to constrain efficiently the design of a robust TML test. Stakes are important in terms of safety and economics since an overestimated value of the CSR has obviously important implications for the shipper.

Acknowledgements

The authors would like to thank Jean-Claude Dupla and Jean Canou, for both the fruitful discussions about liquefaction phenomena and their scientific guidance to the technical design of the experiments. Discussion with Samir Ennour were very helpful. We express our gratitude to Cécile Pradignac, Thierry Douyère and Jean-Marc Devaux for their invaluable technical assistance during the instrumental phases on board. Thanks to André Bodolec who did so much to make all the monitoring system work, and to Armand Lizeur and Vincent Renaud who aided in data processing.

References

Sheng, Y., 2012, Nickel ore end its safe shipment, *Advanced Materials Research Vols 396-398, 2183-2187.*, 638-645.

Spitzlei, M.,2002, Choosing a method for measuring your material's moisture content, *Arnold USA*

IMSBC : *International Maritime Solid Bulk Cargoes Code and Supplement, 2009 – 2011 – 2013*

Valentin, D., 2001. Etude expérimentale des composantes normales des contraintes totales en laboratoire et in situ. *Sciences de l'ingénieur [physics]. Ecole des Ponts ParisTech*.